Effect of removing kupffer cells on nanoparticle tumor delivery

Anthony J. Tavares[a,b,1], Wilson Poon[a,b,1], Yi-Nan Zhang[a,b,1], Qin Dai[a,b], Rickvinder Besla[c], Ding Ding[a,b,2], Ben Ouyang[a,b,d], Angela Li[c], Juan Chen[e], Gang Zheng[e,f], Clinton Robbins[c,g], and Warren C. W. Chan[a,b,h,i,j,3]

[a]Institute of Biomaterials and Biomedical Engineering, University of Toronto, Toronto, ON M5S 3G9, Canada; [b]Terrence Donnelly Centre for Cellular and Biomolecular Research, University of Toronto, Toronto, ON M5S 3E1, Canada; [c]Toronto General Research Institute, University Health Network, Toronto, ON M5G 1L7, Canada; [d]MD/PhD Program, Faculty of Medicine, University of Toronto, Toronto, ON M5S 1A8, Canada; [e]Princess Margaret Cancer Centre, University of Toronto, Toronto, ON M5G 1L7, Canada; [f]Department of Medical Biophysics, University of Toronto, Toronto, ON M5G 1L7, Canada; [g]Peter Munk Cardiac Centre, University Health Network, Toronto, ON M5G 1L7, Canada; [h]Department of Chemistry, University of Toronto, Toronto, ON M5S 3H6, Canada; [i]Department of Chemical Engineering, University of Toronto, Toronto, ON M5S 3E5, Canada; and [j]Department of Materials Science and Engineering, University of Toronto, Toronto, ON M5S 3E1, Canada

[1]A.J.T., W.P., and Y.-N.Z. contributed equally to this work.

[2]Present address: State Key Laboratory of Chemo/Bio-Sensing and Chemometrics, College of Chemistry and Chemical Engineering, College of Biology, Collaborative Innovation Centre for Chemistry and Molecular Medicine, Hunan University, Changsha 410082, China.

[3]To whom correspondence should be addressed. Email: warren.chan@utoronto.ca.

Supporting Information

Materials and Reagents

All buffers and reagent solutions were prepared using deionized water with resistivity of 18.2 MΩ. Phosphate buffered saline (PBS) and 10× tris-borate EDTA buffer (TBE) 10× solutions were obtained from Bio Basic Canada Inc. (Markham, ON, Canada). PBS buffers were autoclaved prior to use. (Reagents used in the synthesis, surface modification and characterization of nanoparticles included: gold (III) chloride trihydrate ($HAuCl_4 \cdot 3H_2O$) (99.9% trace metals basis), sodium citrate tribasic dihydrate (99.0% ACS grade), hydroquinone (99.5% ReagentPlus), sodium bicarbonate (99.7% ACS grade), agarose (low EEO), chloroform (>99% anhydrous), tris(2-carboxylethyl)phosphine hydrochloride (TCEP), and Ficoll® PM 400 were purchased from Sigma Aldrich® (Oakville, ON Canada) and used without further purification. Alexa Fluor® 750 carboxylic acid succinimidyl ester (A750-NHS) and 1,1'-dioctadecyl-3,3,3',3'-Tetramethylindodicarbocynanine, 4-chlorobenzenesulfonate salt (DiD) were from Invitrogen (ThermoFisher Scientific, Carlsbad, CA). Sulfo-Cyanine5 maleimide was purchased from Click Chemistry Tools (Scottsdale, AZ). Methoxy terminated poly(ethylene glycol) thiol (5 kDa) 5KmPEG-SH, amine terminated- poly(ethylene glycol) thiol (10 kDa) 10KamPEG-SH, orthopyridyldisulfide 5kDa PEG succinimidyl valerate 5KOPSS-PEG-SVA, and 5kDa methoxy terminated succinimidyl valerate 5KmPEG-SVA were purchased from Laysan Bio, Inc. (Arab, AL) and Rapp Polymere (Tübingen, Germany), respectively. Corning™ Matrigel™ Membrane Matrix used in tumor xenograft inoculation was obtained from Fisher Scientific Company (Ottawa, ON, Canada). Tween® 20 (TW20) (biotechnology grade), 4-(2-hydroxyethyl)-1-piperazineethanesulfonic acid (HEPES) (biotechnology grade) and sodium chloride (reagent grade) were purchased from BioShop Canada Inc. (Burlington, ON, Canada). Reagent grade nitric

acid (HNO_3) and hydrochloric acid (HCl) were purchased from Caledon Laboratories Ltd., (Caledon, ON, Canada). Elemental gold standard (1000 µg/mL in 2% HCl) was obtained from High-Purity Standards (Charleston, SC). Reagents used in mammalian cell culture included: Fetal bovine serum (FBS) (US certified), Dulbecco's Modified Eagle Medium (DMEM), Roswell Park Memorial Institute (RPMI 1640) medium, and trypsin (0.25% w/v) were purchased from Gibco®, ThermoFisher Scientific (Burlington, ON, Canada). Penicillin-Streptomycin solution (10 000 units/mL) was from FroggaBio Inc. (Toronto, ON, Canada). Clodronate liposomes (5 mg/mL suspension) and PBS liposomes were purchased from ClodronateLiposomes.com (Amsterdam, The Netherlands).

Synthesis of Gold Nanoparticles

The synthesis of 15 nm AuNPs was done using the Frens method (1). Briefly, 100 µL of a 10% (w/v) aqueous solution of $HAuCl_4$ solution was diluted in 100 mL of deionized water. The solution was stirred and heated to a boil, after which 1 mL of 3% (w/v) sodium citrate solution was rapidly injected into the flask. Stirring and heating was maintained for an additional 10 min and then the flask was immediately cooled on ice. The as synthesized 15 nm AuNPs were used as nucleation centers to seed the growth of the larger 50-200 nm AuNPs used in the study. The synthesis of 50-200 nm AuNPs was done as described previously by our group (2). In brief, the appropriate mole equivalents of $HAuCl_4$ (2.5×10^{-2} M), sodium citrate (1.5×10^{-2} M) sodium citrate and the as synthesized 15 nm AuNPs ($2\text{-}4 \times 10^{-9}$ M) were diluted into 100-500 mL of deionized water depending on the reaction scale. Under vigorous stirring conditions, the appropriate volume of hydroquinone (2.5×10^{-2} M) was rapidly injected into the solution at room temperature and the reaction was further stirred overnight. The next day, the AuNP reaction mixtures were stabilized by adding Tween® 20 to a final concentration of 0.05% (v/v) and the solutions were stirred for an

additional 15 min. AuNPs were then purified from excess reagents and precursor by centrifugation between 200-9000 g depending on their respective size. AuNP pellets were concentrated and washed once more in 0.02% (w/v) sodium citrate and subsequently centrifuged. The AuNP concentrates were stored at 4 °C until further use.

Surface Modification of Gold Nanoparticles

The surface of the AuNPs was grafted with a mixed PEG film to enable fluorescent tracking of the AuNPs *in vivo* (3) and to passivate their surface against the adsorption of proteins in serum. Aliquots of stock AuNP concentrates were centrifuged and washed twice with 0.02% (w/v) sodium citrate. The AuNP pellet was re-suspended in 500 µL of deionized water and mixed with a solution containing 5KmPEG-SH and 10KamPEG-SH at a 4:1 mole ratio and at density of 5 PEG·nm^{-2} where the surface area of the AuNP was approximated as a sphere (3). The solution was placed in a heat bath at 60 °C for 1h. The PEGylated AuNPs were purified from excess ligands by centrifugation (400-1800g) and washed twice in 0.1 M sodium bicarbonate (pH 8.4). The PEGylated AuNPs were reacted with a two-fold molar excess of A750-NHS relative to the amount of 10KamPEG-SH initially mixed with AuNPs in 0.1M $NaHCO_3$. The reaction was allowed to proceed overnight on an agitator and was protected from ambient light. A750-tagged AuNPs were purified by centrifugation (400-1800g) and washed once in 0.1M $NaHCO_3$, once in 1× PBS + 0.05% (v/v) TW20, and finally twice in sterile 1× PBS.

Gold Nanoparticle Characterization

Citrate stabilized and PEGylated AuNPs were characterized using transmission electron microscopy (TEM), dynamic light scattering (DLS), zeta potential measurements, UV-visible

absorbance and fluorescence spectroscopy, and agarose gel electrophoresis. The inorganic core sizes of the AuNPs were measured on copper support grids (Ted Pella Inc., Redding, CA) using a Hitachi H-7000 transmission electron microscope at an operating voltage between 50-100 kV. The average inorganic diameter was determined from TEM images containing more than 100 nanoparticles that were sequentially counted using Image J software (National Institutes of Health, Bethesda, MD). The size distribution histogram from each nanoparticle were fit as Gaussian distributions to determine the average inorganic diameter (Figure S1). The hydrodynamic diameter and the zeta potential of the AuNPs were measured using a Malvern Nano ZS zetasizer (Malvern Instruments Ltd., Malvern, United Kingdom). Measurements were made in 0.02% w/v sodium citrate solution, 10 mM HEPES + 1 mM NaCl pH 7.4 (HEPES buffer) or in 1× PBS. For citrate stabilized 15 nm AuNPs, the particles were measured as synthesized without further purification or dilution into buffer. The concentration of the AuNPs was determined from UV-VIS absorbance measurements using a Shimadzu UV-1601PC spectrophotometer, where the size-dependent scaling of the extinction coefficient was calculated as described elsewhere (5). To characterize the coupling of A750 to the AuNPs, steady state fluorescence measurements were made using a Horiba FluoroMax-3 spectrofluorimeter (HORIBA Instruments Inc., Albany, NY). Samples were excited at 740 nm and emission was collected from 750-850 nm. To track the step-wise ligand exchange and coupling of A750 to the AuNPs, agarose gel electrophoresis was used to qualitatively identify charge induced changes in electrophoretic mobility during the ligand exchange protocol. AuNPs stabilized with citrate, the mixed PEG ligands, and those conjugated with A750 were mixed in a 6:1 ratio with Ficoll® PM 400 and were loaded on a 0.7 % (w/v) agarose gel casted in 0.5× TBE. The gel was immersed in 0.5× TBE and run for 35 min at an applied field strength of 13.5 $V \cdot cm^{-1}$. Agarose gels were imaged using a Kodak multispectral in vivo imager using an

excitation of 730 nm and collecting emission at 790 nm over a total exposure time of 1 min. White light images of agarose gels were taken using a standard smart phone camera.

Surface Modification of Silica Nanoparticles

Amine-terminated 100 nm silica nanospheres (SiNPs) were purchased from nanoComposix (San Diego, CA). Aliquots (1 mL) of stock SiNPs were centrifuged at 3000g for 25 min and the supernatant was discarded. The SiNP pellet was resuspended in 10 mM HEPES buffer (1 mM NaCl, pH 7.4) and bath sonicated for 5 min. The nanoparticle suspension was then mixed with 4:1 ratio of 5KmPEG-SVA and 5KOPSS-PEG-SVA, respectively at 5-10 PEG·nm^{-2} and placed in a heat bath at 60°C for 1h. The SiNPs were then purified from excess ligands by centrifugation at 3000g for 25 min. The supernatant was discarded and the pellet was washed in HEPES buffer once more. The SiNPs were resuspended in HEPES buffer and the terminal disulfide was reduced by addition of TCEP to a final concentration *ca.* 5-10 mM at 60 °C for 1h. SiNPs were then centrifuged at 3000g for 25 min and washed once with HEPES buffer. The purified SiNPs were rendered fluorescent by mixing with sulfo-Cyanine5 maleimide (100 µg for each 1 mL aliquot of stock SiNPs) overnight on a mechanical rotator. The following day the solution was centrifuged at 3000g for 25 min and the supernatant was discarded. The SiNPs were washed twice more in PBS and then loaded on an Illustra NAP-25 size-exclusion column (GE Healthcare, Mississauga, ON, Canada). The eluted SiNPs were concentrated using 30 kDa centrifugal filters (EMD Millipore - Merck KGaA, Darmstadt, Germany) according to the manufacturer's protocol. Each animal was injected with *ca.* 2-4 × 10^{11} Cy5-SiNPs suspended in 1×PBS.

Surface Modification of Silver Nanoparticles

Citrate stabilized 100 nm silver nanoparticles were purchased from nanoComposix (San Diego, CA). Nanoparticles were concentrated 20× by centrifugation at 1000g for 2h and resuspended in deionized water. The nanoparticle solutions were then mixed with 5KmPEG-SH and 10KamPEG-SH at a 4:1 mole ratio and at density of 5 PEG·nm^{-2}. The mixture was placed at 60°C for 1h and then centrifuged at 1200g for 30 min. The supernatant was discarded and the pellet was resuspended in 0.1 M sodium bicarbonate containing 0.05% w/v Tween 20, washed twice more and then resuspended in 1×PBS. After PEGylation, it was noted that nanoparticles were sensitive to oxidative induced aggregation. AgNPs was filtered through a 0.2 μm prior to administration to animals. Moreover, A750-AgNPs exhibited weak fluorescence (Fig. S9), thus their biodistribution was determined using ICP-MS. The number of AgNPs injected into each animal was *ca.* 0.8-1× 10^{11}.

Synthesis of DiD-Liposomes

Liposomes were synthesized by hydration of mixed lipid films in 1× PBS (6). Fully saturated (18:0), 1,2-distearoyl-*sn*-glycero-3-phosphoethanolamine-N-[methoxy(polyethylene glycol)-5000] ammonium salt (DSPE-PEG) 2.08 mg, (3.6×10^{-7} mols), hydrogenated soybean L-α-phosphatidylcholine (PC) 3 mg, (3.8×10^{-6} mols), cholesterol (Chol) 1 mg, (2.6×10^{-6} mols) and 1,1'-dioctadecyl-3,3,3',3'-Tetramethylindodicarbocynanine, 4-chlorobenzenesulfonate salt (DiD) 0.072 mg, (6.8×10^{-8} mols) were dissolved in chloroform, mixed and then lyophilized overnight. The following day, 400 μL of 1×PBS was added to the mixed lipid film, vortexed and then subject to five freeze/thaw cycles from -196°C to 60°C. The duration of each freeze or thaw step was 5

min. Crude liposomes were then homogenized to an average diameter of 100 nm using a mini-extruder Avanti Polar Lipids (Alabaster, AL) equipped with a 0.1 µm nucleopore track-etched membrane filter Whatman® (Sigma Aldrich, Oakville, ON, Canada) sandwiched between two filter support discs Avanti Polar Lipids (Alabaster, AL). The liposome mixture was extruded through the membrane a total of 21 passes. Liposomes were stored at 4°C for maximum of 48 h prior to use. Liposomes were characterized using dynamic light scattering, zeta potential measurements and fluorescence spectroscopy. Injection aliquots were prepared by diluting a total of 50 µL of the stock liposome solution to 150 µL using sterile PBS. The concentration administered to each animal was 0.031 $mg \cdot g^{-1}$ based on the total quantity of lipid injected.

Supplementary Figures

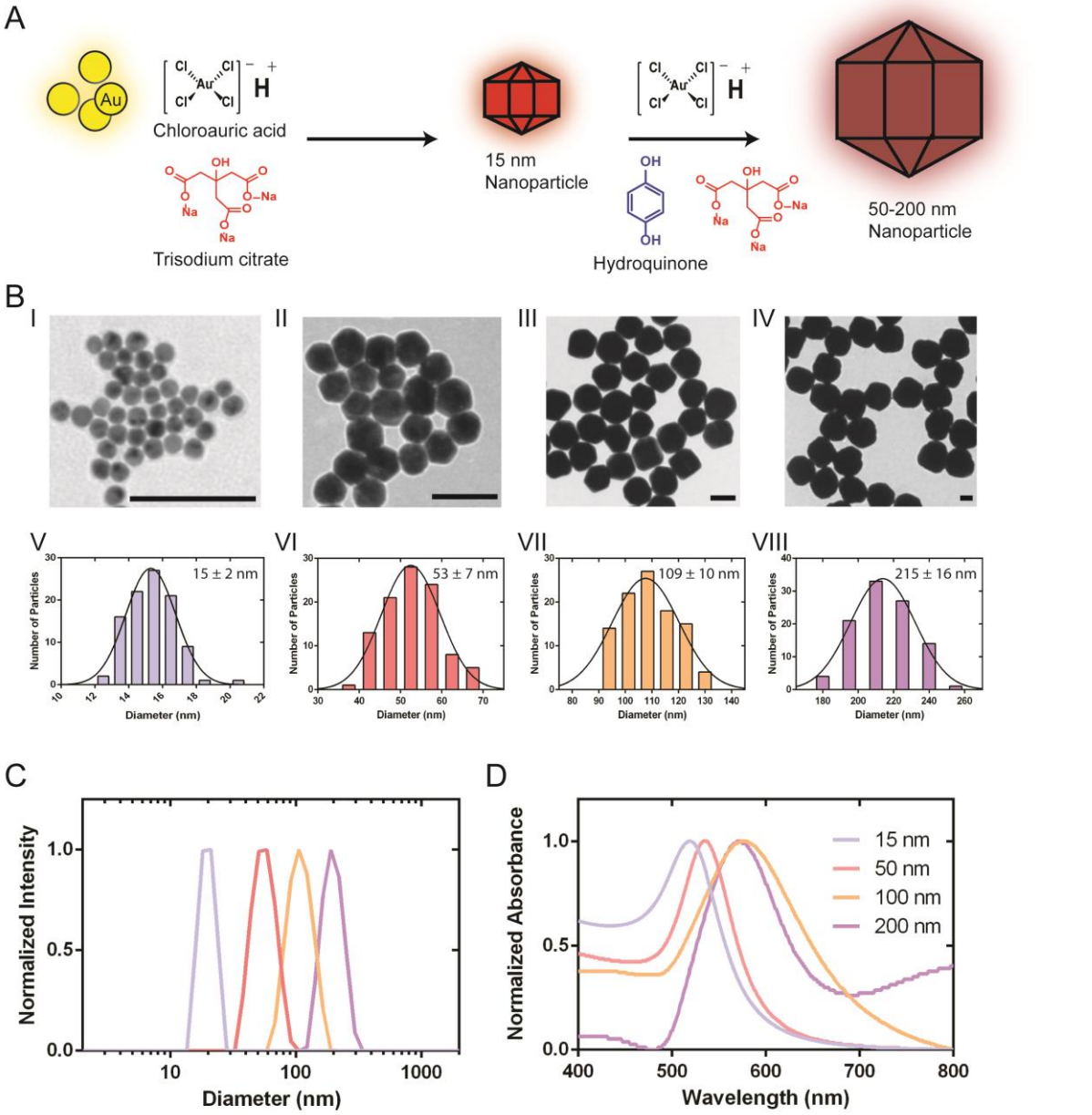

Fig. S1. A Scheme for the synthesis of 15 nm AuNPs that seed the growth of larger 50-200 nm AuNPs. Chloroauric acid is reduced by citrate at reflux to produce 15 nm AuNP seeds. The purified 15 nm AuNP seeds are further reduced to larger 50-200 nm AuNPs with hydroquinone at room termperature in the presence of additional citrate and chloroauric acid. **B** TEM images of (I) 15, (II) 50, (III) 100, and (IV) 200 nm AuNPs, the scale bar in each image is 100 nm. (V-VIII) Corresponding average diameters as determined by fitting a Gaussian to each measured nanoparticle distribution. Average NP diameter was determined by measuring 90-100 NPs from a single TEM frame. The scale bar in each figure is 100 nm The hydrodynamic diameter and the extinction spectra of the 15-200 nm AuNPs is given by **C** and **D**, respectively.

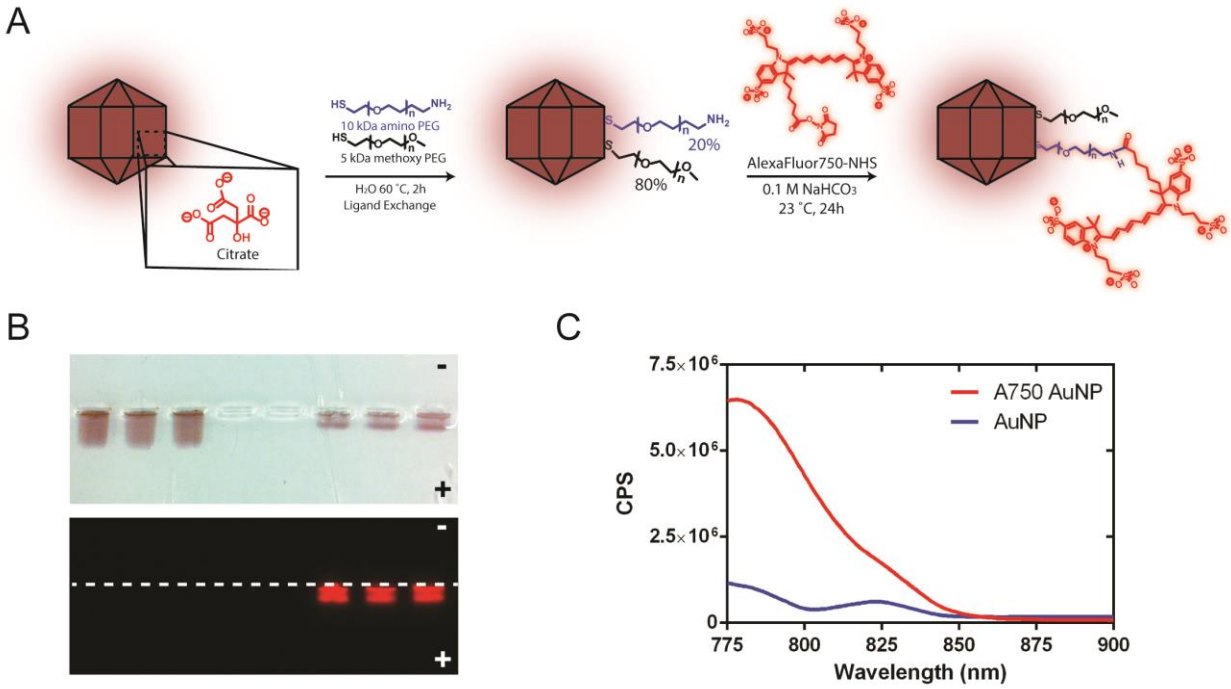

Fig. S2. A Surface modification of AuNPs. Citrate capped AuNPs are ligand exchanged with thiolated 5kDa mPEG and 10kDa amino-PEG at a 4:1 ratio. The free amine facilitated the covalent attachment of Alexa-750 to render the NPs fluorescent. **B** Agarose gel electrophoresis of 100 nm citrate capped (left) and A750 AuNPs (right). The panel below is the same agarose gel fluorescently imaged at 830 nm after excitation with 750 nm light. **C** Solution phase fluorescence measurements of 100 nm A750-AuNPs (red) and citrate AuNPs (blue).

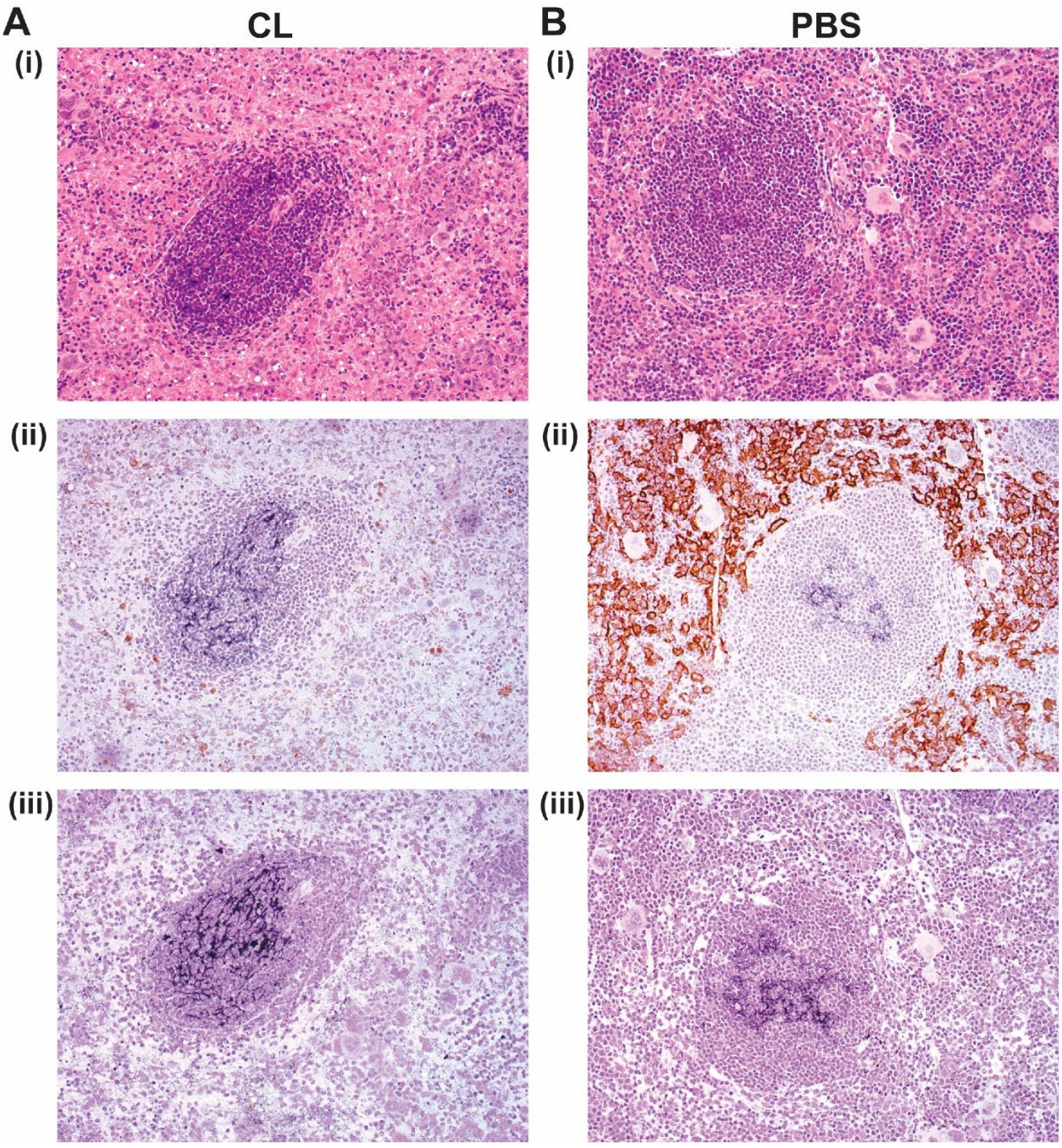

Fig. S3. Histopathology of CD1 *nu/nu* mice splenic tissue 48h after administration of clodronate liposomes **A** and PBS liposomes **B**. The panels shown in **(i)** are tissue slices (H&E) stained. The reduced hematoxylin staining in panel **A (i)** demonstrates a reduction of cells in the red-pulp space. The immunohistochemical staining of the same tissue slice with anti-F4/80-HRP **(ii)** illustrates the depletion of macrophages in the red-pulp space in **A(ii)** from **B(ii)**. The tissue slices shown by **A(iii)** and **B(iii)** are stained with silver nitrate to show the location of AuNPs which appear in the white pulp region in both animals treated with clodronate liposomes and PBS liposomes. The dose of clodronate liposomes was 0.05 $mg \cdot g^{-1}$.

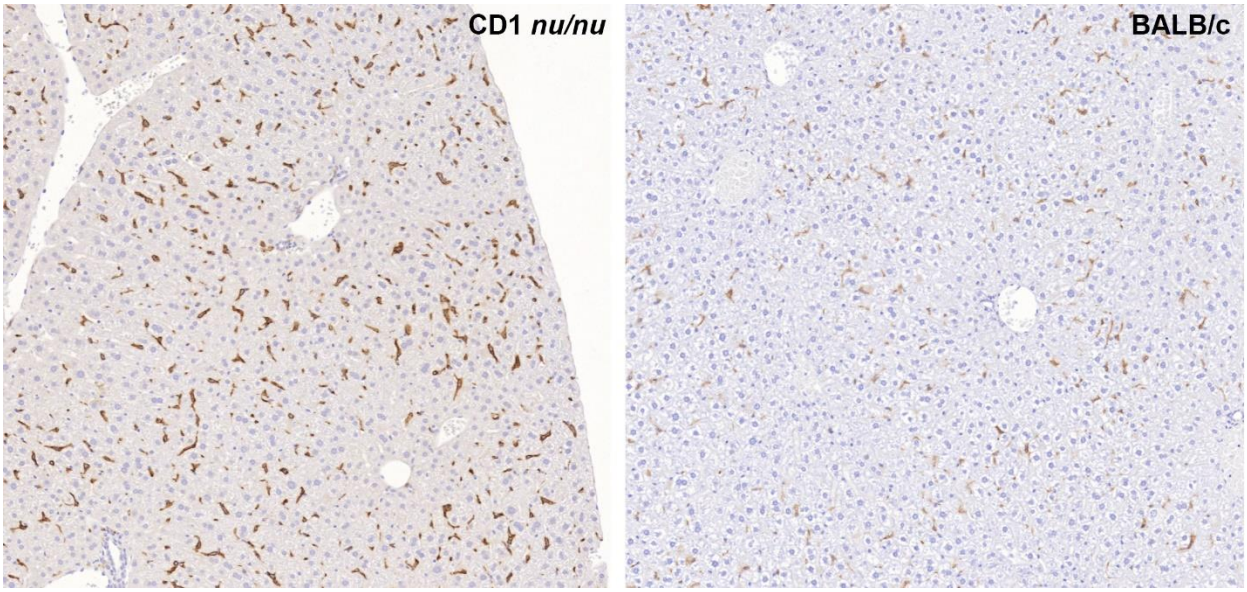

Fig. S4. Histology slices of liver tissue stained with anti-F4/80 HRP from CD1 *nu/nu* mice (left) and BALB/c mice (right). Animals were injected with PBS liposomes 48h prior to isolation and fixation of resected livers. The histological sections qualitatively illustrate a higher density Kupffer cells in CD1 *nu/nu* hepatic tissue as compared to BALB/c. The data is also consistent with the complete hepatic depletion seen of BALB/c livers when animals were injected with a clodronate liposomes dose of 0.017 $mg \cdot g^{-1}$.

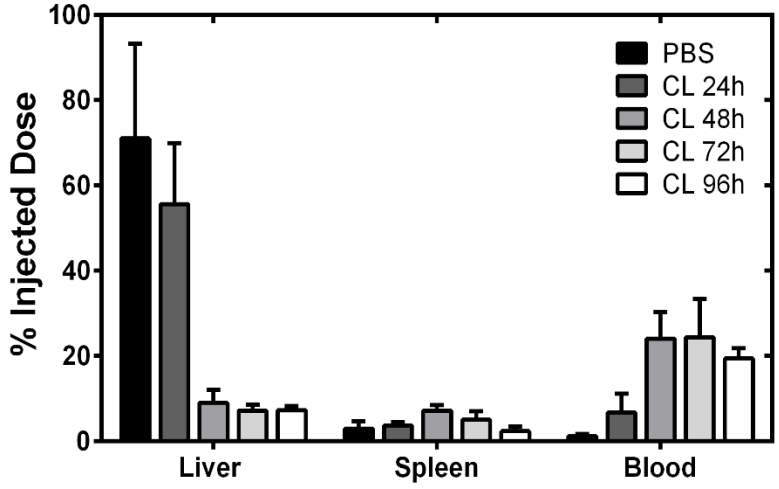

Fig. S5. Evaluation of the delay time between the injection of clodronate liposomes and AuNPs. The AuNP accumulation in the liver, spleen and that remaining in the blood was used assess the degree of macrophage depletion from clodronate liposomes. It was found that 48h after administration of 0.05 $mg \cdot g^{-1}$ clodronate liposomes, complete depletion of Kupffer cells and splenic macrophages minimized the accumulation of AuNPs in these organs and maximized the amount of available AuNPs in the blood.

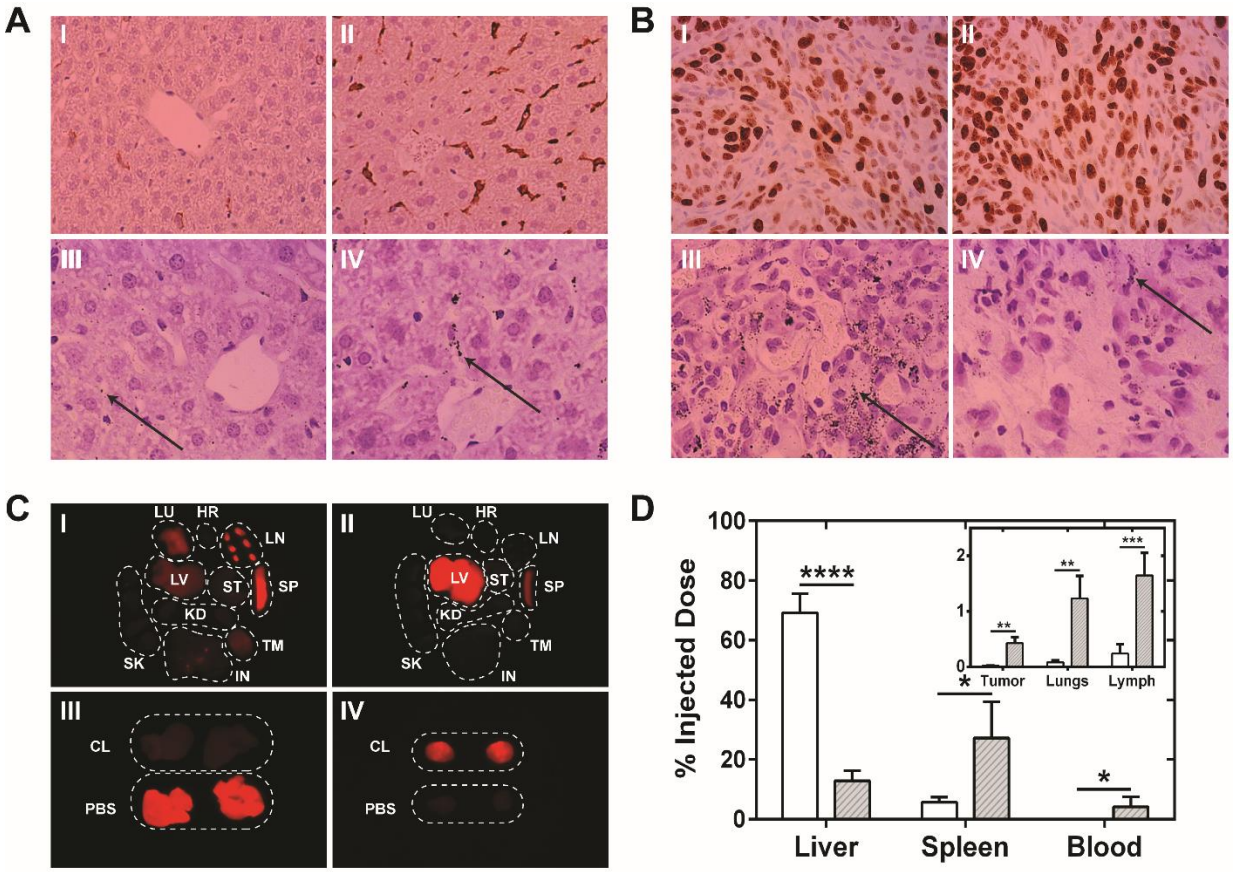

Fig. S6. A Histological sections of liver tissue from CD1 *nu/nu* SKOV3 xenografts after injection of AuNPs. Images (I+III) and (II+IV) are stained with hematoxylin/eosin and silver, respectively. The top two panels are tissue slices from an animal that was administered clodronate liposomes while those on the bottom are respective of pretreatment with PBS liposomes. Increased liver tissue distribution of AuNPs are seen in (IV) as qualitatively illustrated by black clusters characteristic of silver reduction. **B** Histological sections of tumor tissues that were stained with anti-Ki-67/HRP and counter stained with hematoxylin (I+III) to illustrate cancer cells while (II+IV) are stained with silver nitrate to visualize AuNPs. Panels (I+II) were tissues taken from an animal that received clodronate liposomes + AuNPs; clusters of AuNPs are visualized as dark smudges (arrows) in the tumor tissue on the contrary to the slice shown in (IV) where no silver reduction is visible. **C** *Ex vivo* fluorescence images of the 24h biodistribution of AuNPs in an animal treated with (I) and without (II) clodronate liposomes. The animal organs: heart (HR), lungs (LU), liver (LV), stomach (ST), spleen (SP), skin (SK), kidneys (KD), tumor (TM), and intestines (IN) are organized similar to their intrinsic anatomical arrangement. Panels (III) and (IV) show the livers and tumors from pretreatment with clodronate (top) and PBS (bottom) liposomes. The qualitative redistribution of the AuNPs from liver sequestration improves the delivery to the solid tumor. **D** The total organ distribution after 24h as measured by ICP-MS with (grey) and without (white) injection of clodronate liposomes. All organs harvested were analyzed, only organs showing statistically significant (p-value < 0.05) differences in quantitative accumulation are shown. The liver signals were reduced 4-times in animals that were administrated clodronate liposomes an increase in accumulation was seen to the spleen, lungs, and axillary, brachial and inguinal lymph nodes (lymph); AuNPs were still in circulation after 24h. Clodronate liposomes administration enabled a 32-times increase in AuNP delivery to the tumor. Statistical significance was measured at *p-value < 0.05, **p-value < 0.01, ***p-value < 0.001, and ****p-value < 0.0001.

Table S1. Average tumor masses resected from each cancer type.

Tumor Model	Average mass (g)
SKOV3	0.51 ± 0.26
MDA-MD-231	0.0078 ± 0.0065
MDA-MB-435	0.43 ± 0.34
PC3	0.77 ± 0.41
A549	0.17 ± 0.21

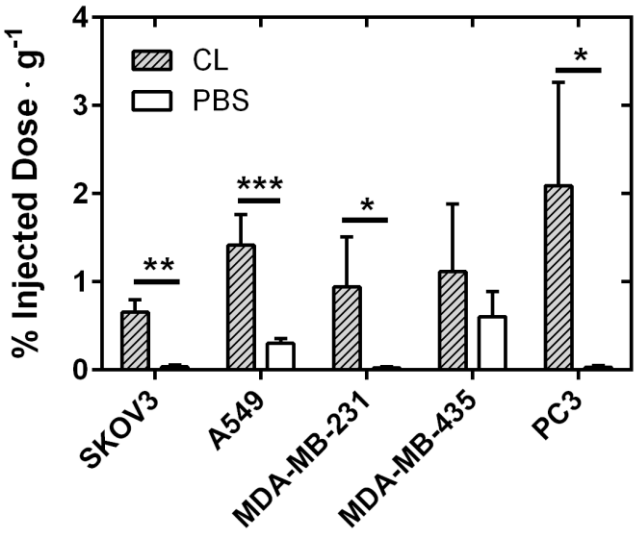

Figure S7. Mass normalized tumor delivery of 100 nm AuNPs (%I.D.·g^{-1}) to various cancer types. The increased accumulation of AuNPs in SKOV3 and A549 subcutaneous xenografts and MDA-MB-231 and PC3 orthotopic xenografts was 20 to 60 times. *p-value < 0.05, **p-value < 0.01, and ***p-value < 0.001.

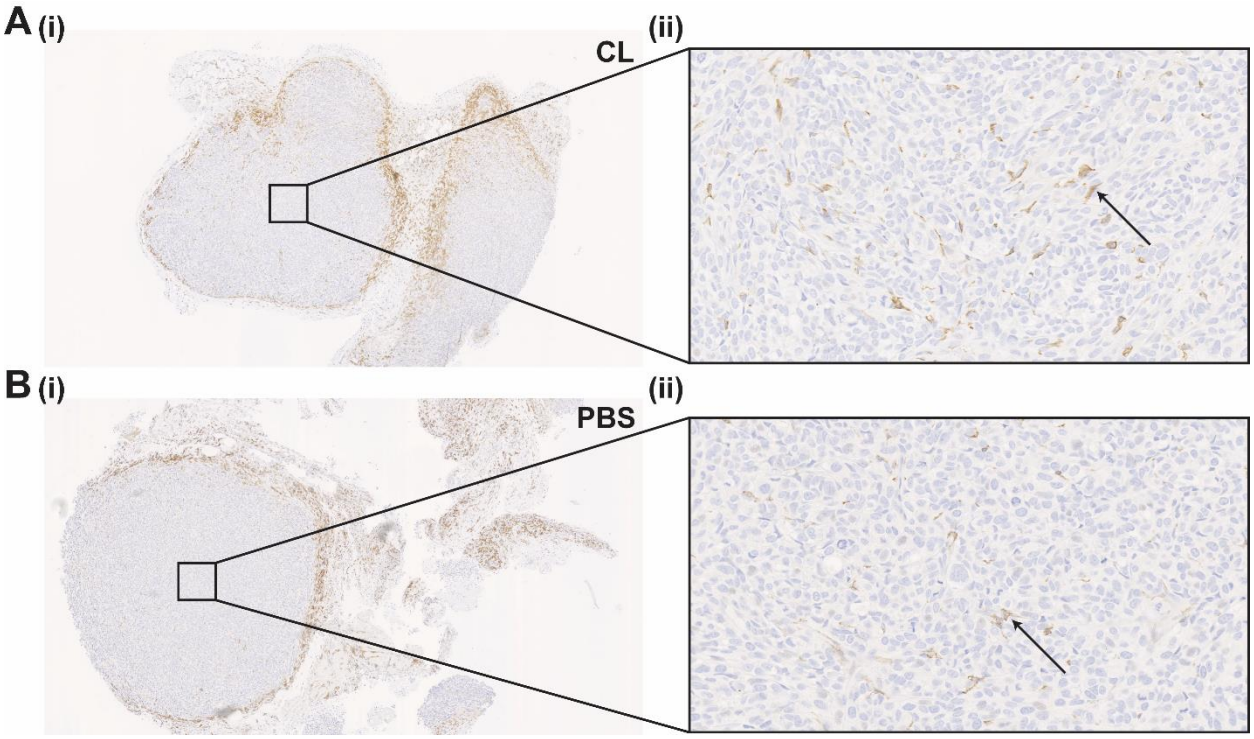

Fig. S8. SKOV3 tumor tissue stained with anti-F4/80 HRP to illustrate tumor associated macrophages. Panels **A (i)** and **(ii)** are images at of a tissue slice at 2.5× and 20× from an animal 48h after injection with clodronate liposomes. Analagous images are shown in **B (i)** and **(ii)** from a control animal treated 48h prior with PBS liposomes. Qualitatively, the tumor associated macrophages that are illustrated by the the brownish-colour (arrows) do not differ in the two tissues. This suggests tumor associated macrophages in the SKOV3 tumor were not depleted with clodronate liposomes at a dose of 0.05 $mg \cdot g^{-1}$.

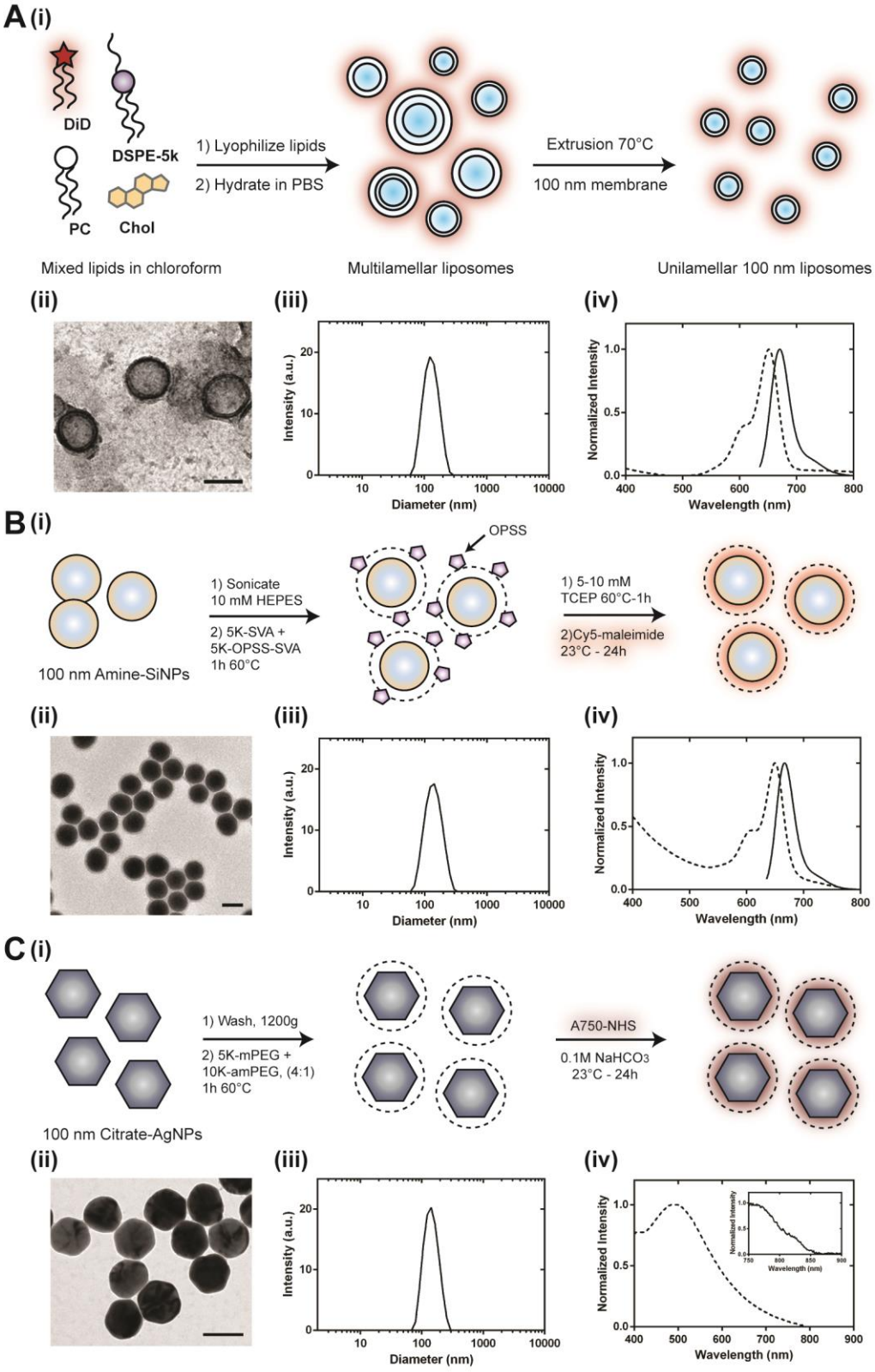

Figure S9.A Synthesis and characterization of nano-liposomes. The synthetic scheme is shown by (i) where mixed lipid films are lyophilized from organic solvents, hydrated in PBS buffer and then crude liposomes are sized and homogenized by extrusion through a 0.1 µm nucleopore membrane. Analysis of nano-liposomes was done by TEM

(ii), DLS (iii) and absorbance/fluorescence spectroscopy (iv). **B** Surface modification of amine terminated SiNPs (i) scheme for derivatization: SiNPs were conjugated with a mixed film of OPSS and methoxy terminated 5kDa PEG ligands. TCEP was used to reduce the OPSS disulfide to a free thiol to conjugate with sulfo-Cy5 maleimide to render the NPs fluorescent. A TEM image, DLS spectrum and absorbance and fluorescence spectra of the modified SiNPs are shown by (ii-iv), respectively. **C** (i) Scheme for the ligand exchange of citrate stabilized AgNPs with methoxy and amine terminated PEG ligands. The terminal amine was used to couple the fluorophore A750-NHS. SiNPs were characterized by TEM (ii), DLS (iii), and absorbance/fluorescence spectroscopy (iv). AgNPs exhibited weak fluorescence, inset in panel C (iv). The scale bar in each TEM image from panels A-C is 100 nm.

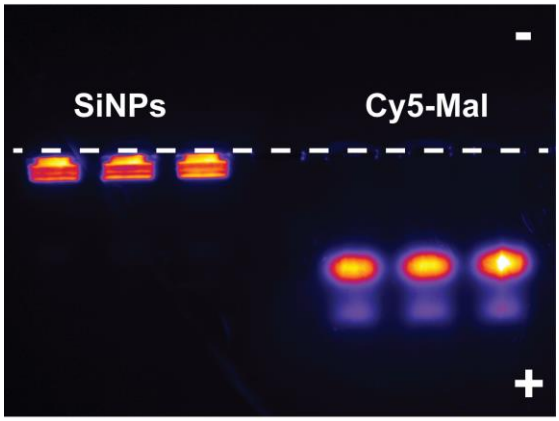

Fig. S10. To confirm the removal of excess Sulfo-Cy5 maleimide, the SiNPs were interrogated against free sulfo-Cy5 maleimide using a 0.7% w/v agarose gel. Samples were run in triplicate, where both displayed anodic migration and confirmed the absence of unconjugated sufo-Cy5 maleimide in the SiNPs samples.

Table S2. Physico-chemical properties of lipsomes, AgNPs, and SiNPs.

Nanoparticle	Inorganic diameter (nm)	Hydrodynamic diameter (nm)	Zeta potential (mV)
DiD-Liposome	-	109.0 ± 8.5	-5.56 ± 0.86
A750-AgNP	96.0 ± 10.0	142.1 ± 9.5	-14.7 ± 0.4
A647-SiNP	101.1 ± 6.2	139.1 ± 9.6	-8.04 ± 0.33

Table S3. Liver biochemistry panel from C57BL/6 mice treated with clodronate liposomes.

	Clodronate liposome dose ($mg \cdot g^{-1}$)				**Reference (mean ± SD)***
	0	**0.005**	**0.017**	**0.05**	
ALT (u/L)	15.2 ± 0.5	25.2 ± 1.32	32.6 ± 6.88	44.0 ± 3.49	50.53 ± 37.15
AST (u/L)	48.3 ± 3.27	74.0 ± 18.6	106.5 ± 15.6	211.3 ± 23.9	126.54 ± 133.29
ALP (u/L)	128.4 ± 7.65	177.2 ± 9.42	184.8 ± 9.68	334.5 ± 24.1	234.51 ± 93.36
TBIL (mg/dL)	0.14 ± 0.02	0.12 ± 0.01	0.10 ± 0.02	0.12 ± 0.04	0.28 ± 0.1

*__Reference from:__ http://www.criver.com/files/pdfs/rms/c57bl6/rm_rm_d_c57bl6n_mouse.aspx (4)

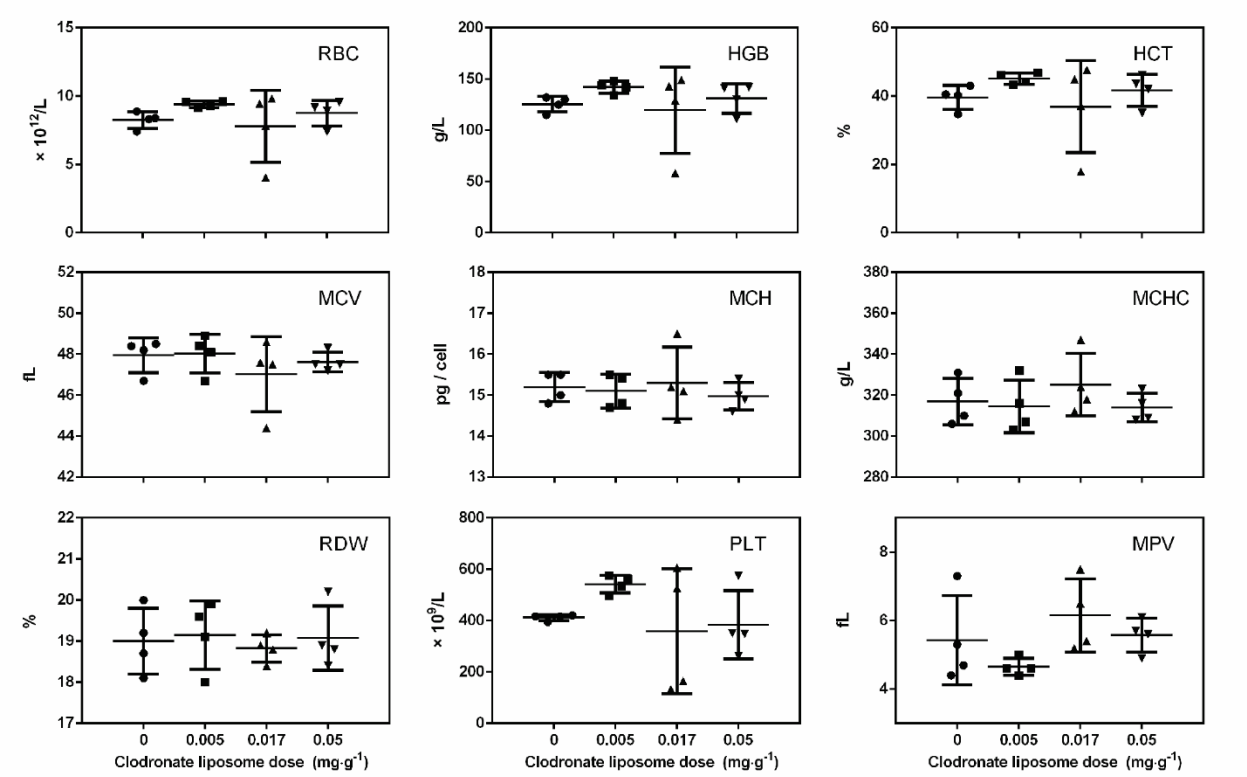

Fig. S11. Hematology analysis of C57BL/6 mice 48h after intravenous injection of clodronate liposomes from 0-0.05mg·g^{-1}. Error bars represent standard deviation calculated from four animals. Parameters shown include red blood cell count (RBC), hemoglobin (HGB), hematocrit (HCT), mean corpuscular volume (MCV), mean corpuscular hemoglobin (MCH), mean corpuscular hemoglobin concentration (MCHC), red blood cell distribution width (RDW), platelet count (PLT), and mean platelet volume (MPV). No statistical significance was observed between treatment groups for all parameters as analyzed by one-way ANOVA with Bonferroni correction ($\alpha = 0.05$).

Table S4. Hematology analysis from C57BL/6 mice treated with clodronate liposomes.

	Clodronate liposome dose (mg·g^{-1})				**Reference (mean ± SD)***
	0	**0.005**	**0.017**	**0.05**	
RBC (M/µL)	8.26 ± 0.61	9.40 ± 0.23	7.79 ± 2.64	8.76 ± 0.95	9.17 ± 1.05
HGB (g/dL)	12.55 ± 0.76	14.20 ± 0.59	11.98 ± 4.20	13.10 ± 1.44	13.72 ± 1.59
HCT (%)	39.6 ± 3.5	45.1 ± 1.6	36.9 ± 13.4	41.7 ± 4.7	45.32 ± 6.27
MCV (fL)	47.95 ± 0.84	48.03 ± 0.94	47.03 ± 1.82	47.63 ± 0.47	49.46 ± 3.88
MCH (pg/cell)	15.20 ± 0.36	15.10 ± 0.41	15.30 ± 0.88	14.98 ± 0.33	15.02 ± 1.11
MCHC (g/dL)	31.70 ± 1.13	31.45 ± 1.29	32.53 ± 1.53	31.4 ± 0.70	30.54 ± 3.19
RDW (%)	19.00 ± 0.80	19.15 ± 0.84	18.83 ± 0.33	19.08 ± 0.78	17.90 ± 1.24
PLT (K/µL)	412 .00 ± 11.46	542.25 ± 34.46	357.50 ± 243.31	384.00 ± 133.85	1167.12 ± 306.96
MPV (fL)	5.43 ± 1.31	4.65 ± 0.25	6.15 ± 1.07	5.58 ± 0.50	4.90 ± 0.33

*__Reference from:__ http://www.criver.com/files/pdfs/rms/c57bl6/rm_rm_d_c57bl6n_mouse.aspx (4)

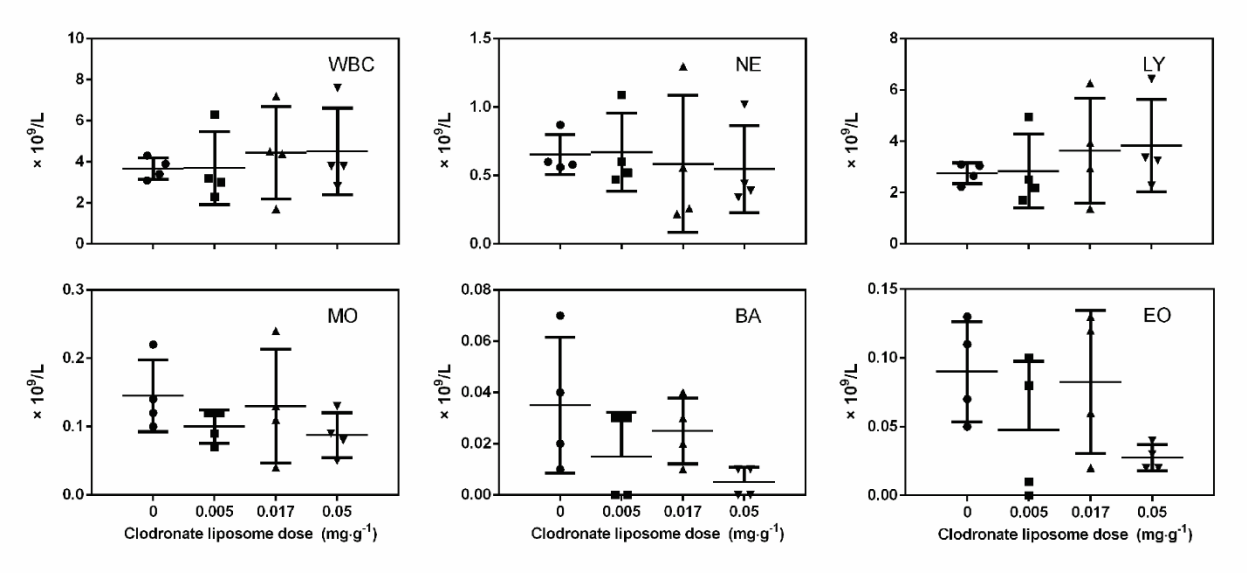

Fig. S12. Analysis of immune cells from blood of C57BL/6 mice 48h after intravenous injection of clodronate liposomes 0-0.05mg·g^{-1}. Error bars represent standard deviation calculated from four animals. Parameters shown include white blood cells (WBC), neutrophils (NE), lymphocytes (LY), monocytes (MO), basophils (BA), and eosinophils (EO). No statistical significance was observed between treatment groups for all parameters as analyzed by one-way ANOVA with Bonferroni correction ($\alpha = 0.05$).

Table S5. Immune cell counts from C57BL/6 mice treated with clodronate liposomes.

	Clodronate liposome dose (mg·g^{-1})				**Reference (mean ± SD)***
	0	**0.005**	**0.017**	**0.05**	
WBC (K/µL)	3.68 ± 0.53	3.70 ± 1.78	4.45 ± 2.25	4.50 ± 2.12	8.69 ± 2.44
NE (K/µL)	0.65 ± 0.15	0.67 ± 0.29	0.59 ± 0.50	0.55 ± 0.32	1.22 ± 0.51
LY (K/µL)	2.76 ± 0.41	2.84 ± 1.44	3.63 ± 2.05	3.83 ± 1.79	6.92 ± 1.92
MO (K/µL)	0.15 ± 0.05	0.10 ± 0.02	0.13 ± 0.08	0.09 ± 0.03	0.37 ± 0.15
BA (K/µL)	0.04 ± 0.03	0.02 ± 0.02	0.03 ± 0.01	0.01 ± 0.01	0.03 ± 0.04
EO (K/µL)	0.09 ± 0.04	0.05 ± 0.05	0.08 ± 0.05	0.03 ± 0.01	0.16 ± 0.13

*__Reference from:__ http://www.criver.com/files/pdfs/rms/c57bl6/rm_rm_d_c57bl6n_mouse.aspx (4)

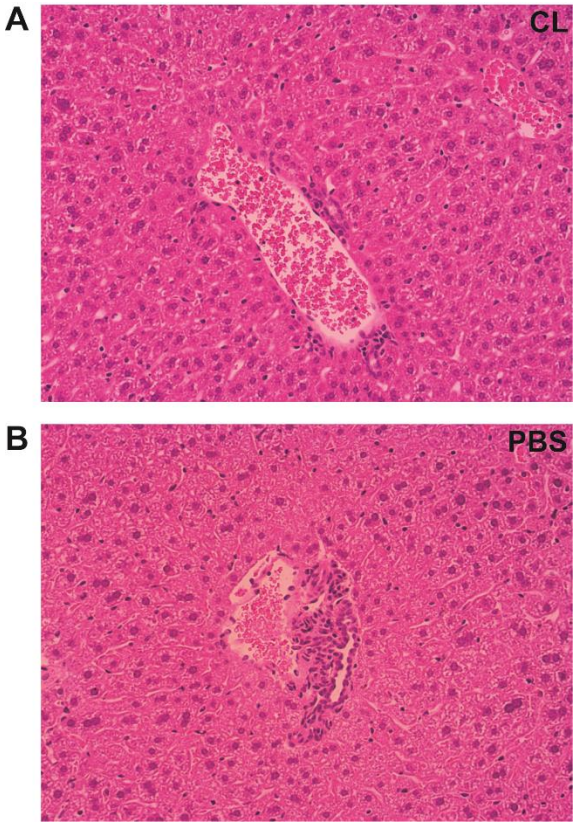

Fig. S13. CD1 *nu/nu* hepatic tissue stained with hematoxylin and eosin (H&E) from an animal treated with clodronate liposomes **A** and control PBS liposomes **B** after 48h. Clodronate liposomes were not seen to cause any gross inflammation to hepatic tissue in comparison to controls.

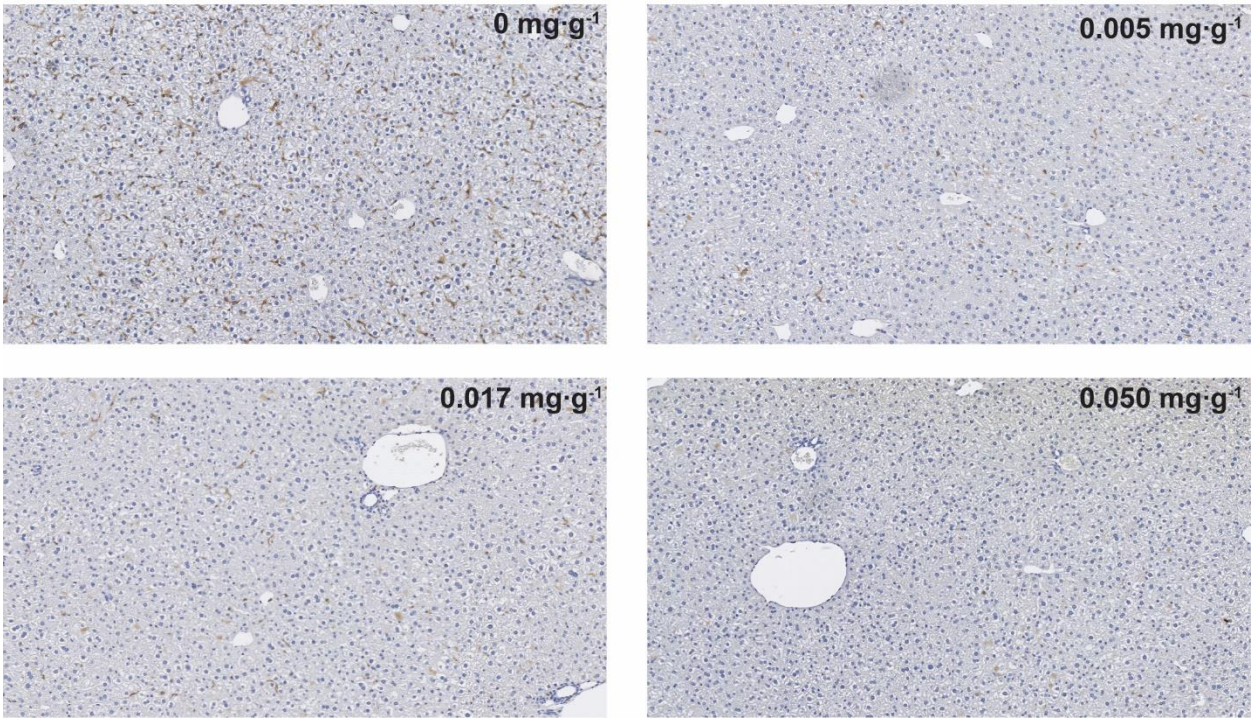

Fig. S14. Immunohistochemically stained tissue sections with anti-F4/80-HRP and counterstained with hematoxylin from livers of C57BL/6 mice treated with clodonate liposomes 0-0.05mg·g^{-1}. The data show a similar dose-dependent depletion of Kupffer cells in hepatic tissue as seen for CD1 *nu/nu* mice.

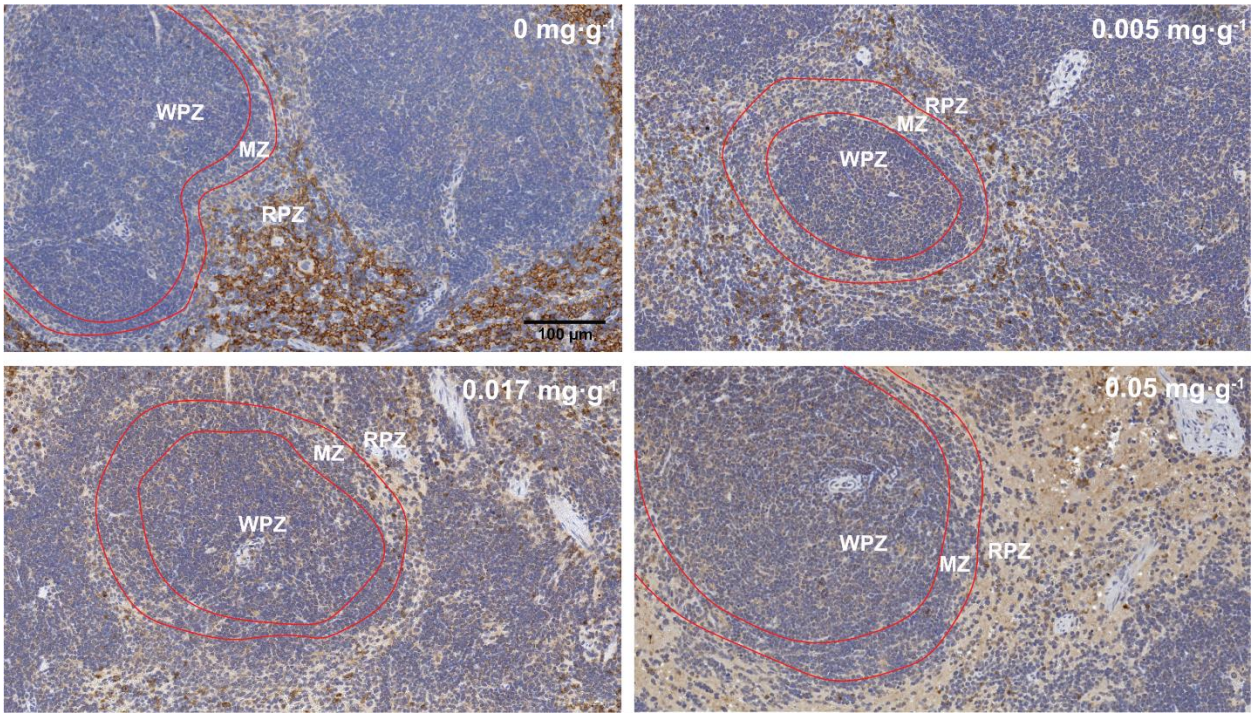

Fig. S15. Immunohistochemically stained splenic tissue sections with anti-F4/80-HRP and counter stained with hematoxylin from C57BL/6 mice treated with clodonate liposomes 0-0.05mg·g^{-1}. The white-pulp zone (WPZ), marginal zone (MZ) and red-pulp zone (RPZ) can be spatially resolved in the tissue sections. Panels A-D show a similar dose-dependent, successive decrease in the quantity of red-pulp macrophages. This dose-dependent depletion of red-pulp macrophages is consistent with what was seen for CD1 *nu/nu* mice.

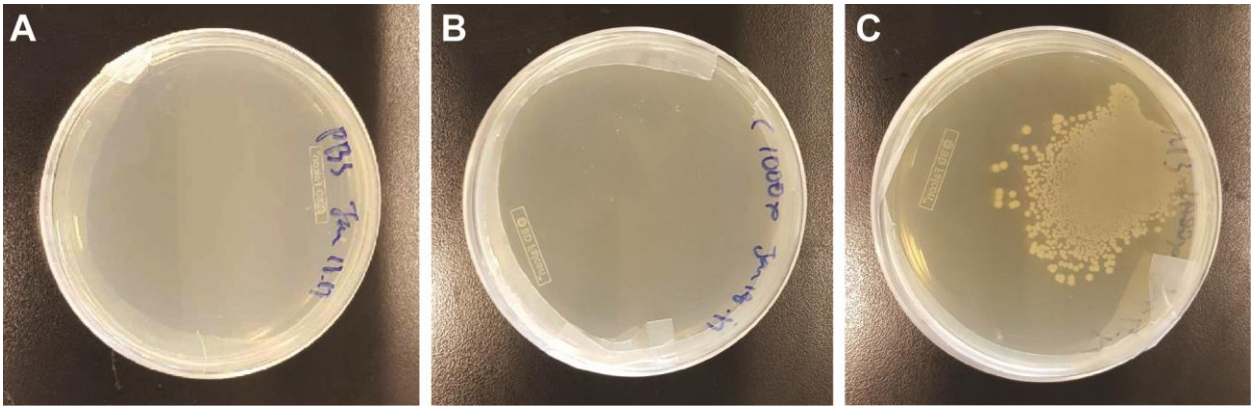

Fig. S16. To confirm induction of sepsis in C57BL/6 after the cecal ligation and puncture procedure, bacteria cultures were done by plating sterile PBS (A), blood from sterile animals (n=4) (B) and blood isolated from killed septic animals (n=4) and incubating at 37°C for 24h. (C) Bacterial colony growth can be seen in the agar plate in C, confirming induction of sepsis.

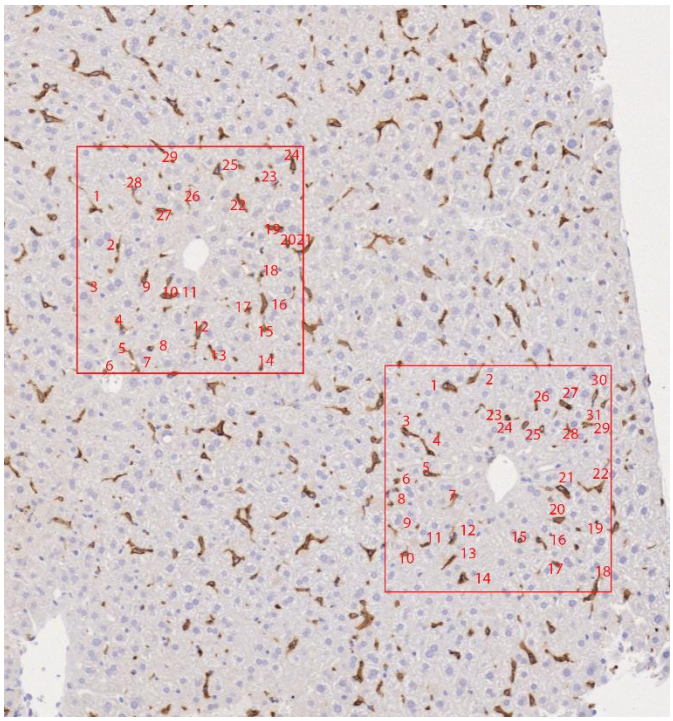

Fig. S17. CD1 *nu*/*nu* hepatic tissue immunohistochemically stained with anti-F4/80 HRP to display Kupffer cells (brownish-red features). The average number of Kupffer cells in hepatic tissue was used to provide a semi-quantitative assessment on the degree of macrophage for a given dose of clodronate liposomes. The number of Kupffer cells in fixed areas centered on either a portal triad or central vein (red box) were counted. The average was computed from three independent areas of each tissue slice.

References

1. Frens G (1973) Controlled nucleation for the regulation of the particle size in monodisperse gold suspensions. Nat Phys Sci (Lond) 241:20–22.

2. Perrault SD, Chan WCW (2009) Synthesis and Surface Modification of Highly Monodispersed, Spherical Gold Nanoparticles of 50-200 nm. *J. Am. Chem. Soc.* 131:17042–17043.

3. Chou LYT, Chan WCW (2012) Fluorescence-Tagged Gold Nanoparticles for Rapidly Characterizing the Size-Dependent Biodistribution in Tumor Models. *Adv. Healthcare Mater.* 1:714–721.

4. Charles River (2011) *Research Models C57BL6 Mice*. http://www.criver.com/files/pdfs/rms/c57bl6/rm_rm_d_c57bl6n_mouse.aspx. Accessed 12-19-2016.

5. Zagorovsky K, Chan WCW (2013) A plasmonic DNAzyme strategy for point-of-care genetic detection of infectious pathogens. *Angew. Chem. Int. Ed.* 52:3168–3171.

6. Abraham SA, Waterhouse, DN, Mayer LD, Cullis PR, Madden TD, Bally MB (2005) The liposomal Formulation of Doxorubicin. *Methods Enzymol.* 391:71-97.